JOURNAL OF APPLIED ELECTROCHEMISTRY **25** (1995) 642–650

Surface pH measurements during nickel electrodeposition

J. JI, W. C. COOPER, D. B. DREISINGER, E. PETERS

Department of Metals and Materials Engineering, The University of British Columbia, Vancouver, BC, V6T 1Z4, Canada

Received 4 May 1994; 20 November 1994

To better understand the electrochemistry of nickel electrowinning from nickel chloride solutions at the cathode–electrolyte interface, the cathode surface pH was measured using a flat-bottom combination glass pH electrode and a 500 mesh nickel-plated gold gauze as cathode. The cell was a modification of that designed by Romankiw and coworkers. The pH electrode was positioned at the back of, and in direct contact with, the gauze cathode. As expected, the cathode surface pH was always higher than the pH in the bulk electrolyte, and if the current density was sufficiently large, it could cause the precipitation of insoluble $Ni(OH)_{2(5)}$ on the cathode surface. Lower bulk pH, higher nickel concentration, higher temperature, and the additions of H_3BO_3 and NH_4Cl effectively suppressed the rise of the cathode surface pH. The results provide further evidence of the buffering action of H_3BO_3 and NH_4Cl and of the enhancement of nickel deposition by H_3BO_3. At current densities less than 240 $A\,m^{-2}$ additions of NaCl and Na_2SO_4 suppressed the rise of the cathode surface pH but to a much smaller degree.

1. Introduction

The electrodeposition of nickel often does not proceed at 100% current efficiency. The balance of the current is consumed normally in hydrogen evolution. Because of this hydrogen evolution, the hydrogen ion is depleted in the electrolyte near the cathode surface. Therefore, the pH of the electrolyte near the cathode surface is always higher than that in the bulk electrolyte.

There are three basic factors that can suppress the increase of the cathode surface pH. The first factor is the mass transfer rate of hydrogen ions towards the cathode surface. In this regard, the reduced thickness of the diffusion layer brought about by vigorous agitation will prevent to a large extent the cathode surface pH from rising. The second factor is the proton donating pH buffers, such as boric acid, or the bisulfate ion. The third factor is the hydroxyl-consuming pH buffers, such as $NiOH^+$, $Ni_4(OH)_4^{4+}$. As the cathode surface pH increases, the following equilibria will shift to the right to generate more protons:

$$HSO_4^- \longrightarrow SO_4^{2-} + H^+ \tag{1}$$

$$Ni^{2+} + H_2O \longrightarrow NiOH^+ + H^+ \tag{2}$$

$$4Ni^{2+} + 4H_2O \longrightarrow Ni_4(OH)_4^{4+} + 4H^+ \tag{3}$$

$$Ni^{2+} + 2H_3BO_3 \longrightarrow Ni(H_2BO_3)_2 + 2H^+ \tag{4}$$

$$Ni^{2+} + NH_4^+ \longrightarrow Ni(NH_3)^{2+} + H^+ \tag{5}$$

When the supply of hydrogen ions is unable to meet the depletion rate, the cathode surface pH will rise and eventually lead to the formation of insoluble nickel hydroxide on the cathode surface, a condition which must be avoided during nickel electrowinning.

Ovari and Rotinyan [1] measured the cathode surface pH using a microglass pH electrode during nickel electrodeposition under the conditions of 0.25–2 M $NiCl_2$, 55 °C and pH 0.75–2.5. They found that the surface pH was always higher than the bulk pH if the bulk pH was above 1.5. They claimed that the surface pH increased initially with increasing current density; however, it did not increase further when the current density reached a certain level.

Kuhn and Chan [2] reviewed the reliability of surface pH measurements during nickel electrodeposition using different techniques. Each technique, as they pointed out, had certain drawbacks associated with the effect of gas bubbles and the current flow. The most convenient technique was to use a pH-sensing electrode, such as black Pt/H_2, Pt-quinhydrone, Sb_2O_3/Sb and glass pH electrodes, among which the glass pH electrode was the most widely used. The use of the glass pH electrode with a flat bottom was not mentioned. They proposed new techniques which are not easily feasible, such as using an optically-transparent electrode together with a u.v.–visible indicator.

A useful technique for measuring the surface pH, which has been employed with modifications in the present study, is to use a flat-bottom glass pH electrode juxtaposed with a fine gold gauze cathode [3–6]. In a study carried out in an unstirred dilute nickel chloride (< 0.2 M $NiCl_2$) electrolyte, Deligianni and Romankiw [4] used as the cathode a 2000 mesh gold gauze, having an aperture diameter of 7 μm and a thickness of 5 μm. They found that a higher nickel concentration and the presence of boric acid resulted in a lower surface pH. Using a rotating pH electrode, they observed that the surface pH decreased continuously with increasing rotation

0021-891X © 1995 Chapman & Hall

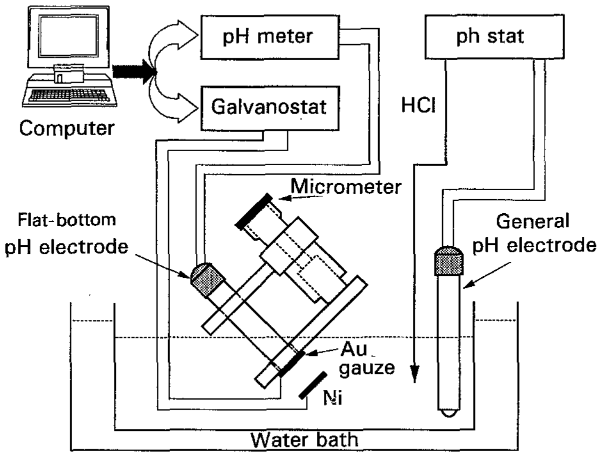

Fig. 1. Schematic drawing of the apparatus for the surface pH measurement and associated equipment.

speed [3]. Their tests were based on a potentiostatic step or linear potential sweep.

The purpose of the present investigation was to extend earlier work on the determination of the pH of the electrolyte near the cathode surface during metal deposition. The research has focused on nickel electrodeposition in the expectation that the results would lead to a better understanding of nickel electrowinning from chloride solutions.

2. Experimental apparatus and conditions

The measurement of the cathode surface pH was carried out using an apparatus constructed in-house. The idea for such an apparatus originated from the work of Romankiw et al. [3–6]. However, a number of modifications were made to their apparatus and experimental procedures. A schematic drawing of the experimental arrangement is shown in Fig. 1. The system consisted of a galvanostat (Solartron 1286 electrochemical interface), pH meter (Radiometer PHM82 standard pH meter), a pH stat (Radiometer ETS822 titration system), a general combination glass pH electrode (Baxter/Canlab) to control the pH of the bulk electrolyte, a special combination glass flat-bottom pH electrode (Orion) to measure the surface pH, a micrometer to adjust the position of the flat-bottom pH electrode, a nickel anode, a gold gauze cathode, and a computer to control the instruments and to take measurements. The whole measuring assembly was placed in the cell at an angle of approximately 45 °. The gold gauze, serving as the cathode, had an exposed diameter of ~ 15 mm. During the experiments the nickel was deposited on the front side of the gold gauze which had been preplated with a layer of nickel. The flat-bottom pH electrode was placed next to the back side of the nickel-plated gold gauze. The distance between the gold gauze cathode and the sensor of the flat-bottom pH electrode could be adjusted using a micrometer. During the measurement, they actually contacted each other. The nickel anode with a diameter ~ 15 mm was placed directly below the gold gauze with a space of ~ 20 mm. The cell contained 250 ml of electrolyte.

The solution was stirred gently with a magnetic stirrer during pH measurement for the sake of uniform bulk pH. The rotational speed of the stirrer was kept at 160 rpm for all of the measurements. The bulk pH was controlled to be constant. Before the experiments, the solution was deaerated with nitrogen for about 20 min to remove dissolved oxygen. Unless otherwise stated, the bare gold gauze was always preplated with a ~ 0.5 μm thick nickel film (by deposition at 50 A m^{-2} for 300 s) before any tests. After each test, the gold gauze was cleaned via anodic dissolution of the previously deposited nickel layer. It has been calculated that gold was a very inert cathode substrate even in nickel chloride solutions [7].

*Table 1. Dimensions of 500 mesh gold gauze**

Estimated from SEM photos			*From manufacturer*†		
Wires diameter /μm	*Space between wires* /μm	*Effective area*‡ /%	*Wire diameter* /μm	*Space between wires* /μm	*Effective area* /%
17.0	33.0	89	11.4	39.4	63

* 1 mesh = 1 line per 2.54 cm.

† The gold gauzes were purchased from Buckbee-Mears Co., 254 E-6th St., 6th floor, St. Paul, MN 55101, USA

‡ Effective area $= \frac{\text{Real area}}{\text{Nominal area}} \times 100$.

The dimensions of the 500 mesh gold gauze used in this work are listed in Table 1, both according to the manufacturer's specifications and those estimated from our SEM photomicrographs. The calculation of the effective area is shown. In terms of the effective area, the 500 mesh gauze was the most suitable among the four gold gauzes which were evaluated. The diameter of the pH sensor of the flat-bottom pH electrode is around 8 mm. For 500 mesh gold gauze, as an example, this pH electrode reflects an average pH value covering twenty thousand $[1/4 \times \pi \times 8000^2/(17.0 + 33.0)^2 \approx 20\,000]$ holes on the gauze surface.

The surface pH was measured as a function of time at a given current density. The deposition time was typically 150 s, and the surface pH values presented were the readings at the end of the experiment or averaged in the stable region. The curves of pH against time were recorded for each run. The surface pH's measured with 500 mesh gold gauze are believed to be a fair representation of the true surface pH. If the flat-bottom pH electrode is brought into direct contact with the gold gauze, the distance between the glass membrane sensor of the pH electrode and the electrochemical reaction sites varies because of the 'mushroom' shape of the wires of the gold gauze. For the 500 mesh gold gauze, the maximum distance from the "mushroom" top of the wires to the membrane sensor is around 36% of the wire diameter (i.e., around 6 μm). This distance is well below the normal diffusion layer thickness which is on the order of 80–300 μm.

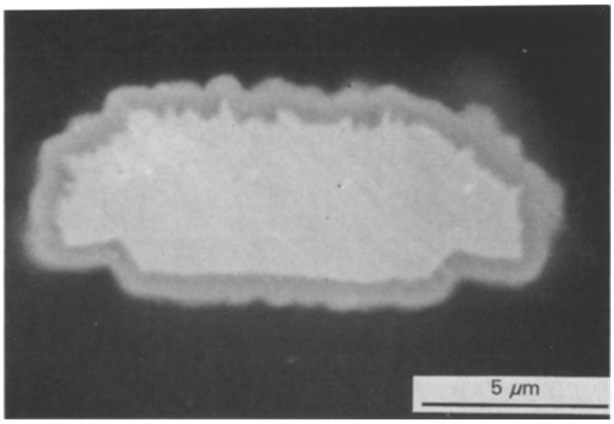

Fig. 2. SEM photomicrograph of 500 mesh gold gauze coated with ~ 1 µm (nominal) thick nickel film (20 kV, 2000×) (cross section).

Practically, we need to know the surface pH values measured on the nickel substrate such as would be encountered in industrial nickel electrodeposition. One way to overcome this problem would be to use a nickel gauze instead of a gold gauze. However, the nickel gauze would be electrochemically active in acidic media and could not be used repeatedly.

For a ~ 1 µm thick coating (Fig. 2), SEM photomicrographs of the cross-section of the wires demonstrate that the substrate surface has been covered completely with the nickel film. The nickel film was deposited uniformly along the contours of the gold substrate surface. If the thickness were decreased by 50%, that is, to 0.5 µm, the surface would still be covered completely with the nickel film. The nickel-coated gold gauze, after nickel was dissolved anodically, was examined by energy dispersive X-ray spectrometry (EDX), Fig. 3(b). This surface exhibited no nickel peaks. Hence one can be sure that using the anodic dissolution method, the deposited nickel film can be completely dissolved anodically by controlling the final potential up to 0.05 V vs SCE.

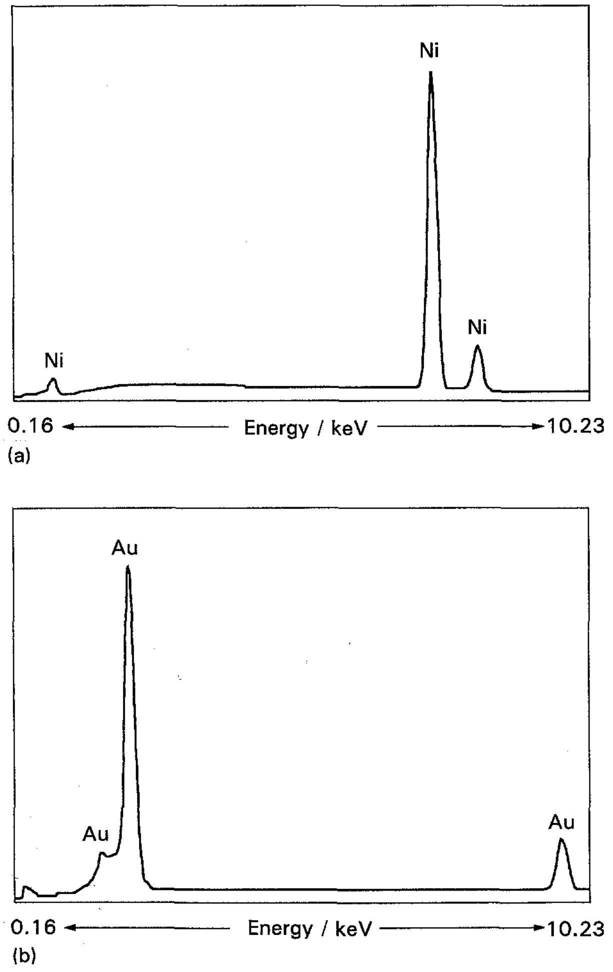

Fig. 3. EDX diagrams of 500 mesh gold gauze coated with nickel layer 1 µm in thickness (a) and after anodic dissolution (b) (20 kV, 7000×).

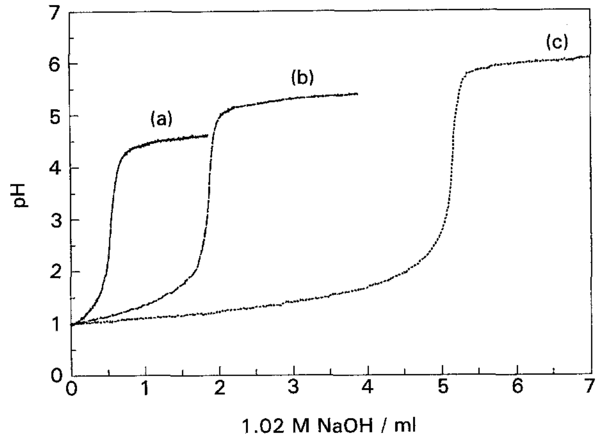

Fig. 4. pH titration curves for different $NiCl_2$ concentrations at 25 °C (150 ml sample and 0.5 ml min^{-1} speed). Key: (a) 3 M $NiCl_2$; (b) 2 M $NiCl_2$; (c) 0·937 M $NiCl_2$.

3. Results and discussion

3.1. *Effect of nickel concentration on the surface pH at 25 °C*

The neutralization curves for different electrolytes obtained by titration with standard NaOH solution serve to indicate the marked difference in the amount of free acid present in solutions having the same initial pH. The titration curves (Fig. 4) show clearly that the amount of sodium hydroxide required to neutralize the free acid at pH 1 decreases dramatically with increasing $NiCl_2$ concentration. The pH at which insoluble nickel hydroxide starts to form also

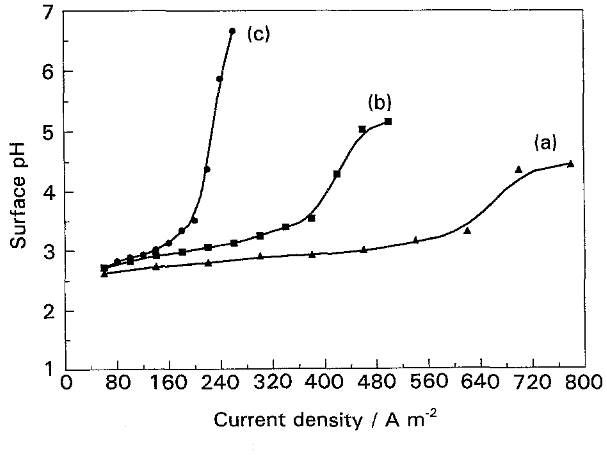

Fig. 5. Surface pH as a function of current density for different $NiCl_2$ concentrations at 25 °C (500 mesh gold gauze and bulk pH 2.5). Key: (a) 3 M $NiCl_2$; (b) 2 M $NiCl_2$; (c) 0.937 M $NICl_2$.

Table 2. The amount of acid released when pH changes from 2.5 to 5.5

Electrolytes	$\Delta[H^+]_T$ (mol)
0.937 M $NiCl_2$	$(10^{-2.5} - 10^{-5.5}) \times 0.250/2.29 = 3.45 \times 10^{-4}$
0.937 M $NiCl_2$ + 0.365 M Na_2SO_4	$(10^{-2.5} - 10^{-5.5}) \times 0.250/1.23 = 6.42 \times 10^{-4}$
0572 M $NiCl_2$ + 0.365 M $NiSO_4$	$(10^{-2.5} - 10^{-5.5}) \times 0.250/0.990 = 7.98 \times 10^{-4}$
0.572 M $NiCl_2$ + 0.365 M $NiSO_4$+ 0.365 M Na_2SO_4	$(10^{-2.5} - 10^{-5.5}) \times 0.250/0.578 = 13.7 \times 10^{-4}$

decreases with increasing $NiCl_2$ concentration. The surface pH's measured in the pure nickel chloride solutions are represented in Fig. 5. As can be seen from Fig. 5, lower surface pH's are observed in the more concentrated nickel chloride solutions. It should be noted that the amount of hydrogen gas formed is directly proportional to the decrease in the amount of hydrogen ions in the solutions. According to the formal definition, $\mathrm{pH} = -\log a_{\mathrm{H}^+} = -\log(\gamma_{\mathrm{H}^+}[\mathrm{H}^+])$ and $-\ln a_{\mathrm{H}^+} = (E - E^{0\prime} - E_{\mathrm{j}})F/RT$, where E is the e.m.f. of the cell, $E^{0\prime}$ is the standard potential, E_{j} is the liquid junction potential [8]. Therefore, when the surface pH is related to the hydrogen evolution, the effect of the activity coefficient of the hydrogen ions must be taken into account. The activity coefficients of the hydrogen ions in 3 M $NiCl_2$ and 2 M $NiCl_2$ at 25 °C were found to be 11.8 and 2.8 times as large as that in 0.937 M $NiCl_2$ solution (27.1, 6.51 and 2.29, respectively) [7].* Thus at a given pH, the concentration of hydrogen ions is considerably smaller in more concentrated nickel chloride solutions. In terms of nickel electrodeposition, this means that a lower bulk pH in the highly concentrated nickel chloride solutions will still result in a high current efficiency such as can be reached only at a higher pH level in less concentrated solutions.

3.2. *Effect of sulfate on the surface pH at 25 °C*

Three sulfate-containing nickel chloride electrolytes were tested, that is, 0.572 M $NiCl_2$ + 0.365 M $NiSO_4$, 0.937 M $NiCl_2$ + 0.365 M Na_2SO_4 and 0.572 M $NiCl_2$ + 0.365 M $NiSO_4$ + 0.365 M Na_2SO_4. As shown in Fig. 6, the presence of the sulfate ion suppresses the rise of the surface pH. However, the differences in the surface pH's at different sulfate concentrations are quite marginal at bulk pH 2.5. The activity coefficients of the hydrogen ions measured previously [7] in these solutions can be used to estimate the change in the amount of total acid† available for 250 ml of the solution as the pH goes from 2.5 to 5.5 (Table 2).

The value 2.29 is the activity coefficient of hydrogen ions in 0.937 M $NiCl_2$, and the values 1.23, 0.990 and 0.578 are the activity coefficients of hydrogen ions in the sulfate-containing nickel chloride solutions 0.937 M $NiCl_2$ + 0.365 M Na_2SO_4, 0.572 M $NiCl_2$ + 0.365 M $NiSO_4$ and 0.572 M $NiCl_2$ + 0.365 M $NiSO_4$ + 0.365 M $NaSO_4$, respectively [7]. The above activity coefficients obtained initially as shown in Fig. 7 were corrected for liquid junction potentials. If the current efficiency of nickel and the thickness of the diffusion layer are assumed to be of the same order of magnitude in these four solutions, the ratio of current densities to reach a surface of pH 5.5 should be around 1 : 1.9 : 2.5 : 4.2. Obviously, the curves in Fig. 6 do not match this ratio. The reason for this, as was found in electrodeposition tests [7], is that the current efficiency of nickel decreases continuously with the increase of sulfate concentration and the decrease of chloride concentration. That is to say, at a given pH and total nickel concentration, the current efficiencies have the order of $\mathrm{CE}_{\mathrm{NiCl_2}} > \mathrm{CE}_{\mathrm{NiCl_2+Na_2SO_4}} > \mathrm{CE}_{\mathrm{NiCl_2+NiSO_4}} > \mathrm{CE}_{\mathrm{NiCl_2+NiSO_4+Na_2SO_4}}$. For instance, at pH 1.5, 60 °C and 200 A m^{-2}, nickel current efficiencies are 97.0%, 95.4%, 93.6% and 91.3%, respectively, for the electrolytes of 0.937 M $NiCl_2$, 0.937 M $NiCl_2$ + 0.365 M Na_2SO_4, 0.572 M $NiCl_2$ + 0.365 M $NiSO_4$, and 0.572 M $NiCl_2$ + 0.365 M $NiSO_4$ + 0.365 M Na_2SO_4.

Accordingly, from the measurements of surface pH and current efficiency, it can be concluded that the addition of sulfate to nickel chloride solutions has the effect of shifting the marked increase in surface pH to a higher current density and reducing the current efficiency of nickel electrodeposition. At pH 2.5, the above calculations (see Table 2) indicate that the total acidity of the solution increases with increasing sulfate concentration. As the pH titration curves in

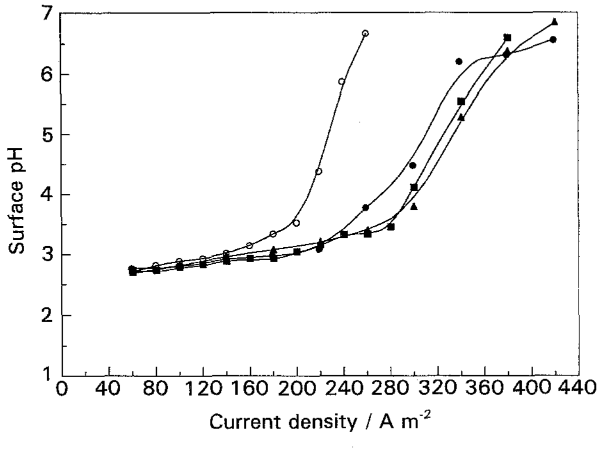

Fig. 6. Surface pH as a function of current density for different sulfate concentrations at 25 °C (500 mesh gold gauze and bulk pH 2.5). Key. (■) 0.572 M $NiCl_2$ + 0.365 M $NiSO_4$; (●) 0.937 M $NiCl_2$ + 0.365 M Na_2SO_4; (▲) 0.572 M $NiCl_2$ + 0.365 M $NiSO_4$ + 0.365 M Na_2SO_4; (○) 0.937 M $NiCl_2$.

---

* The activity coefficients of hydrogen ions in the solutions of 3 M $NiCl_2$, 2 M $NiCl_2$ and 0.937 M $NiCl_2$ were determined experimentally using a combination glass pH electrode by measuring the pH responses to a series of additions of hydrochloric acid solution [7]. The values so obtained were corrected for the liquid junction potentials.

† Here total acid means the concentration of free hydrogen ion plus bisulfate ion.

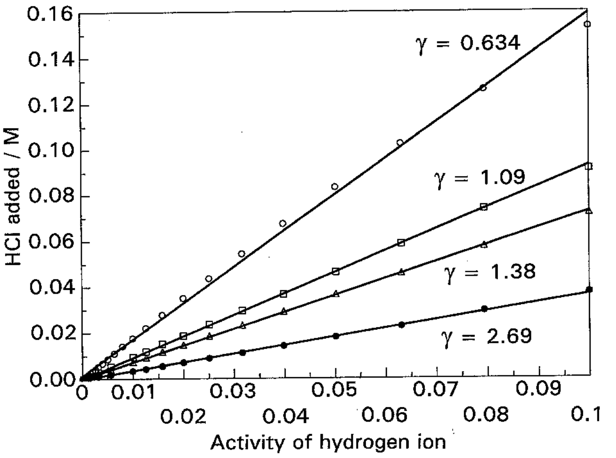

Fig. 7. Concentrations of hydrogen plus bisulfate as a function of hydrogen ion activity in sulfate-containing nickel chloride solutions at 25 °C. Key: (○) 0.572 M $NiCl_2$ + 0.365 M $NiSO_4$ + 0.365 M Na_2SO_4; (□) 0.572 M $NiCl_2$ + 0.365 M $NiSO_4$; (△) 0.937 M $NiCl_2$ + 0.365 M Na_2SO_4; (●) 0.937 M $NiCl_2$.

Fig. 8 show, the amount of total acid at pH 1 for these electrolytes differs markedly.

3.3. *Effect of sodium chloride on the surface pH at 25 °C*

Chloride ions promote the deposition of nickel, conventionally believed to be due to a catalysis of the electron transfer via a so-called 'chloride ion bridge' between Ni^{2+} ions and the cathode surface [9]. Piatti et al. [10] gave another account. They assumed that the nickel surface is not completely free of oxygen-containing species, and believed that it is likely that chloride ion interaction takes place through this kind of layer. We believe that it likely occurs by the overlapping of the chloride ion orbitals, which are distorted by the high local electric field in the electrical double layer, with part of the orbitals of nickel. However, according to one theory, chloride ions enter the hydration sphere of the nickel ions and replace one of the associated water molecules so that the nickel ions are able to move closer to the cathode surface and engage in electron transfer [11]. In electrodeposition studies Ji [7] found that the addition of 2 M NaCl increased the current efficiency of nickel deposition.

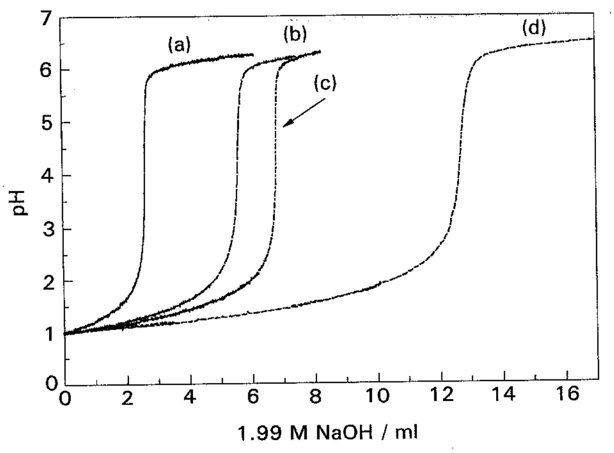

Fig. 8. pH titration for different sulfate concentrations at 25 °C. (150 ml sample; 0.5 ml min^{-1} speed). Key: (a) 0.937 M $NiCl_2$; (b) 0.937 M $NiCl_2$ + 0.365 M Na_2SO_4; (c) 0.572 M $NiCl_2$ + 0.365 M $NiSO_4$; (d) 0.572 M $NiCl_2$ + 0.365 M $NiSO_4$ + 0.365 M Na_2SO_4.

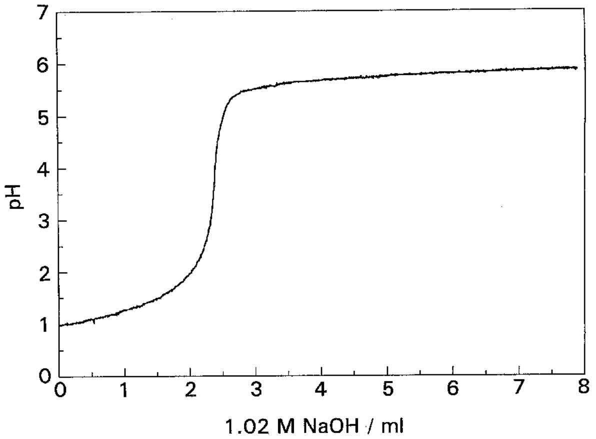

Fig. 9. pH titration for 0.937 M $NiCl_2$ + 2 M NaCl at 25 °C (150 ml sample; 0.5 ml min^{-1} speed).

The pH titration curve in Fig. 9 shows that the free acid concentration of 0.937 M $NiCl_2$ and 2 M NaCl at pH1 is almost one-half that in 0.937 M $NiCl_2$ solution (see Fig. 4). As sodium chloride is a fairly weak complexing agent for nickel and is not a buffering agent at all, the decrease in free acid concentration at pH 1 can be ascribed to the increase in the activity coefficient of the hydrogen ions. The addition of sodium chloride would also increase the activity coefficient of nickel ions but to a lesser extent [7]. The results of surface pH measured for 0.937 M $NiCl_2$–2 M NaCl electrolyte are shown in Fig. 10. The data confirm that the addition of sodium chloride suppresses the rise of the surface pH at current densities less than 240 A m^{-2}.

3.4. *Effect of boric acid on the surface pH at 25 °C*

The function of boric acid in nickel electrodeposition is a controversial subject. The conventional view is that boric acid serves as a pH buffer. However, it has been claimed that boric acid serves as a homogeneous catalyst and lowers the overpotential of nickel deposition [9, 12–14]. It has been reported

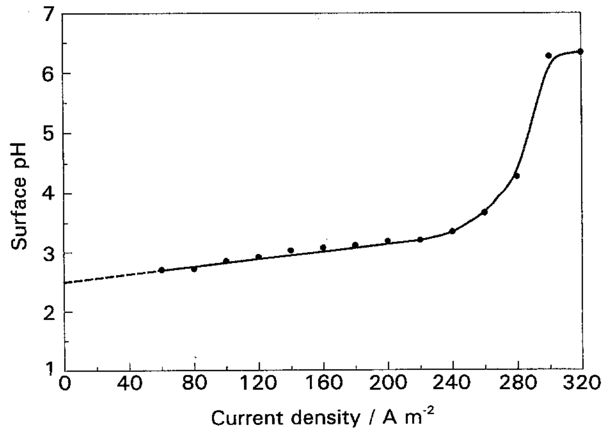

Fig. 10. Surface pH as a function of current density in 0.937 M $NiCl_2$ + 2 M NaCl at 25 °C (500 mesh gold gauze and bulk pH 2.5).

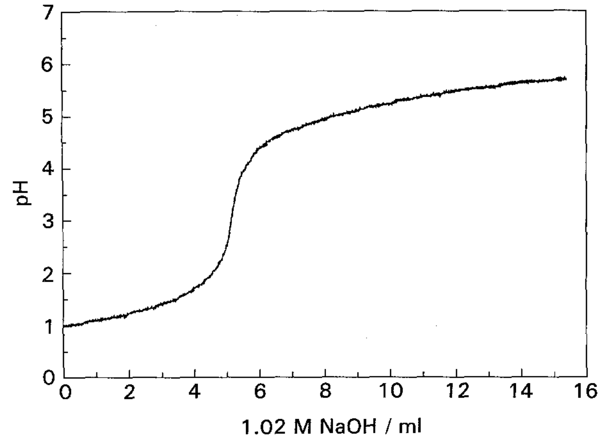

Fig. 11. pH titration for 0.937 M $NiCl_2$ + 0.485 M H_3BO_3 at 25 °C (150 ml sample; 0.5 ml min^{-1} speed).

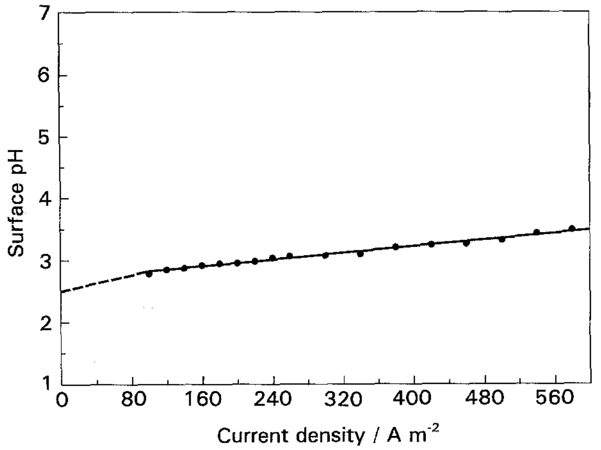

Fig. 12. Surface pH as a function of current density in 0.937 M $NiCl_2$ + 0.485 M H_3BO_3 at 25 °C (500 mesh gold gauze and bulk pH 2.5).

that there is a complex between nickel and borate ions, $Ni^{2+} + 2H_3BO_3 = Ni(H_2BO_3)_2 + 2H^+$, in mixed chloride-sulfate solutions [15]. Another interesting point concerning the buffering capacity of boric acid is the effect of an electric field. It was found that the equilibrium dissociation constant of boric acid near the cathode surface is substantially larger than the corresponding value in the bulk electrolyte [16].

To clarify the function of boric acid in nickel-containing solutions, starting from the simplest case, a series of pH titrations was conducted titrating free boric acid (5 ~ 40 g dm^{-3}) solution in the presence and absence of 2 M NaCl at 25 °C against NaOH solution [7]. There are altogether four species which may exist and their equilibrium reactions are as follows [17]:

$$H_3BO_3 + H_2O \overset{Q_{11}}{=} B(OH)_4^- + H^+ \quad (6)$$

$$2H_3BO_3 \overset{Q_{21}}{=} B_2O(OH)_5^- + H^+ \quad (7)$$

$$3H_3BO_3 \overset{Q_{31}}{=} B_3O_3(OH)_4^- + H^+ + 2H_2O \quad (8)$$

$$4H_3BO_3 \overset{Q_{42}}{=} B_4O_5(OH)_4^{2-} + 2H^+ + 3H_2O \quad (9)$$

The calculations using the equilibrium constants from the literature [17] indicated that multistep dissociation of boric acid would happen as the pH went up to 13. However, interestingly, only the first-step dissociation was evident at pH up to 13 from the pH titration results [7].

The pH titration curve of 0.937 M $NiCl_2$ + 0.485 M H_3BO_3 is shown in Fig. 11. Comparing the titration curves of 0.937 M $NiCl_2$ in Fig. 4, the buffering capacity of the $NiCl_2 + H_3BO_3$ solution increases dramatically and the buffering range of boric acid is extended to the acidic region. This observation is consistent with the formation of a weak complex between nickel and borate ions, which has been reported [15]. By the formation of the nickel-borate complex, $Ni^{2+} + 2H_3BO_3 = Ni(H_2BO_3)_2 + 2H^+$, more hydrogen ions are available in the solution. However, the free acid concentration at pH 1 in 0.937 M $NiCl_2$ + 0·485 M H_3BO_3 is very close to that of 0.937 M $NiCl_2$, indicating that H_3BO_3 does not change the activity coefficient of the hydrogen ions. However, the pH at the peak of the change in pH with NaOH volume (d*p*H/d*V*) is shifted from ~ 4.4 to ~ 2.9 as a result of the addition of H_3BO_3. This also indicates that boric acid starts to form a complex with the nickel ion and thus to produce hydrogen ions when the pH is above ~ 2.9.

The measured surface pH's as a function of current density are given in Fig. 12. The surface pH's are lower than in the case of the $NiCl_2 + NH_4Cl$ electrolyte (Fig. 14) at higher current densities, and increase almost linearly with current density. As can be seen from the pH titration curve, this behaviour at lower surface pH is not just the result of the buffering action of boric acid. It seems that boric acid also enhances the deposition of nickel, which observation appears to be in agreement with the so-called catalytic effect of boric acid. Indeed, higher current efficiencies of nickel were observed in the electrodeposition tests at bulk pH 1.1 and 60 °C [7]. Besides this catalytic effect, to account for the lower surface pH behaviour, it may also be speculated that due to the very sharp pH gradient immediately away from the surface of the gold gauze, as reported by Romankiw [6], the surface pH's measured with the 500 mesh gold

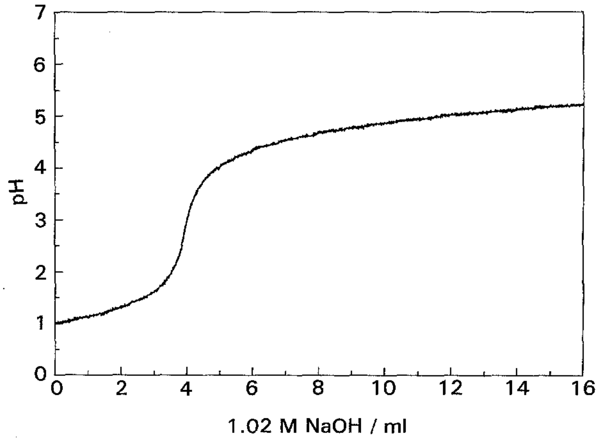

Fig. 13. pH titration for 0.937 M $NiCl_2$ + 1.31 M NH_4Cl at 25 °C (150 ml sample; 0.5 ml min^{-1} speed).

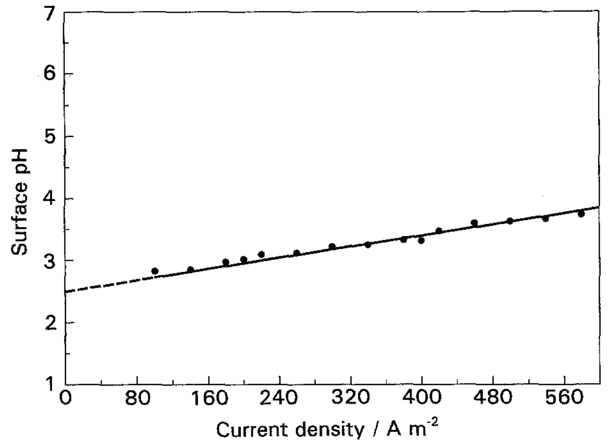

Fig. 14. Surface pH as a function of current density in 0.937 M $NiCl_2$ + 1.31 M NH_4Cl at 25 °C (500 mesh gold gauze and bulk pH 2.5).

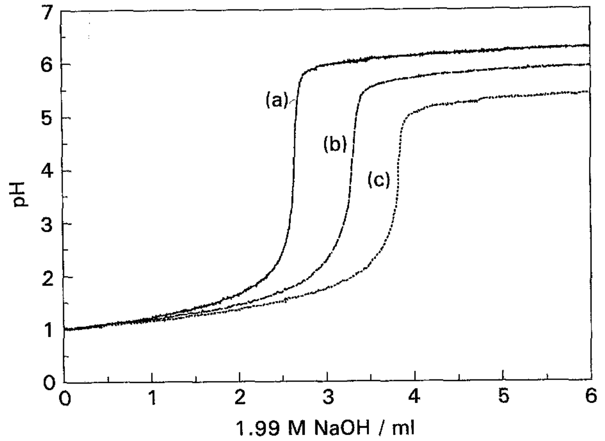

Fig. 15. pH titration for 0.937 M $NiCl_2$ at different temperatures (150 ml sample; 0.5 ml min^{-1} speed). Key: (a) 25 °C; (b) 40 °C and (c) 60 °C.

gauze are still different to a certain degree from the real surface pH's. Therefore, boric acid may indeed play a significant buffering role there even though it is not apparent from the titration curve.

3.5. *Effect of ammonium chloride on the surface pH at 25 °C*

The addition of ammonium sulfate or chloride is indispensable to nickel powder production via electrolysis at extremely high current densities [18–22]. Ammonium chloride is both a strong complexing agent and a pH buffer. As with boric acid, the buffer point of free ammonium chloride is in the basic region around pH 9.3. However, the formation of strong nickel-ammonia complexes, $Ni^{2+} + xNH_4^+ \rightarrow Ni(NH_3)_x^{2+} + xH^+$, shifts this buffering range to a relatively acidic region.

Bjerrum [23] studied the nickel ammine complexes in 2 M NH_4NO_3 and 1 M NH_4Cl at 30 °C. He found that the number of NH_3 molecules bound to the Ni^{2+} ion increased with increasing NH_3 concentration, starting from $Ni(NH_3)^{2+}$ up to $Ni(NH_3)_6^{2+}$. It has been calculated [7] that nickel monoammine complex $Ni(NH_3)^{2+}$ should begin to form at pH above 3.2 in the electrolyte 0.937 M $NiCl_2$ + 1.31 M NH_4Cl.

By comparing the titration curves of $NiCl_2 + NH_4Cl$ (Fig. 13) and $NiCl_2 + H_3BO_3$ (Fig.11), the pH at peak dpH/dV is similarly close to ~ 2.9, but NH_4Cl has a much stronger buffering action. Compared with that of pure $NiCl_2$ solution, the free acid concentration at pH 1 decreased as a result of the addition of NH_4Cl. As with the addition of boric acid, when NH_4Cl is added, the surface pH is also low (~ 2.8 at 100 A m^{-2}) and increases almost linearly with current density (Fig. 14). This means that NH_4Cl is also quite effective in moderating the surface pH at a low level in nickel electrodeposition.

3.6. *Effect of temperature on the surface pH*

As a starting point, three pH titrations were carried out on 0.937 M $NiCl_2$ solution at 25, 40 and 60 °C in order to reveal the change of the electrolyte pH with temperature. The curves shown in Fig. 15 reveal two things. First, the free acid at a given pH increases with temperature. Second, the pH at which the insoluble nickel hydroxide starts to form decreases with increasing temperature. In other words, the activity coefficient of the hydrogen ions decreases with temperature, and a high temperature favours the precipitation of nickel hydroxide.

The surface pH measurements at 40 and 60 °C were conducted using exactly the same apparatus and almost the same procedures as those employed at 25 °C. One exception was for tests at 60 °C, where the solutions were not deaerated before measurements and not agitated during measurements in order to simulate the practical situation. Measurements at 40 °C without agitation were also performed for the sake of comparison. Certain difficulties were encountered at higher current densities as the gold gauze easily cracked when a thick layer of nickel was deposited on it. This phenomenon generally happened when the current density exceeded 1000 A m^{-2} and the electrodeposition ran for more than 100 s. The charge passed during this period would produce a nickel deposit of a nominal thickness of 3.6 μm. Because of this problem, measurements were restricted to current densities up to 1000 A m^{-2} for 100 s of electrodeposition for each run.

The measured surface pH's in 0.937 M $NiCl_2$ at a bulk pH of 2.5 and temperatures of 25, 40 and 60 °C are presented in Fig. 16. Several observations are to be noted from this graph. First, high temperature does enhance significantly the rate of nickel reduction so that there is a lower surface pH. Second, agitation lowers effectively the surface pH by increasing the mass transfer rate of hydrogen ions towards the cathode surface. Third, the final surface pH's are consistent with the pH titrations, indicating that the formation of insoluble nickel hydroxide on the cathode surface should be expected at these high pH levels. It should be mentioned that there is a nickel concentration polarization during nickel electrodeposition, so that the pH at which the insoluble nickel hydroxide starts to precipitate should be

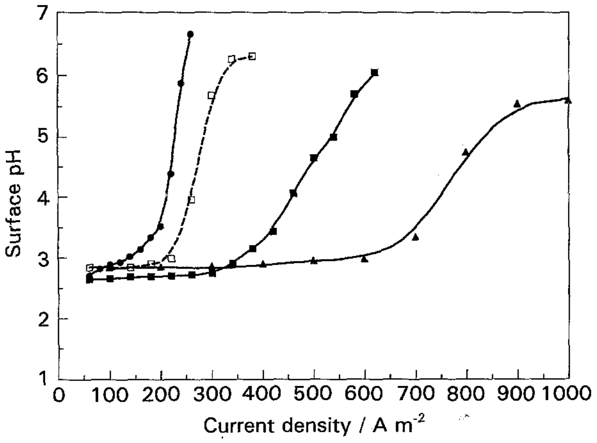

Fig. 16. Surface pH as a function of current density in 0.937 M $NiCl_2$ at different temperatures (500 mesh gold gauze and bulk pH 2.5). Key: (●) 25 °C, stirring; (□) 40 °C, no stirring; (■) 40 °C, stirring; (▲) 60 °C, no stirring.

somewhat higher than that estimated from the titration curves or from the solubility product based on the bulk nickel concentration.[‡]

Another interesting point shown in Fig. 16 is that at 60 °C without agitation the surface pH is about 0.34 unit higher than the bulk pH even at a current density as low as 100 A m^{-2}. Agitation was indeed found to affect the surface pH even under no current passage when a layer of nickel was present on the surface of the gold gauze. This higher surface pH at low current densities under no agitation is believed due to the chemical attack by hydrogen ions and the effect of dissolved oxygen.

3.7. *Nickel speciation in chloride solutions*

Since the nature of the nickel species in chloride solutions as a function of pH is of importance in understanding nickel electrodeposition from such solutions, the principal results of Ji's studies on this subject are summarized here [7].

In the acidic region, Ji found that the predominant nickel species are Ni^{2+}, and $NiCl^+$ in pure $NiCl_2$ solutions and Ni^{2+}, $NiCl^+$ and $NiSO_4$ in the mixed sulfate-$NiCl_2$ solutions. The concentration of $NiOH^+$ is negligible. All the other species such as $Ni(OH)_{2(aq)}$, $Ni(OH)_3^-$, $Ni(OH)_4^{2-}$, Ni_2OH^{3+} and $Ni_4(OH)_4^{4+}$ are negligible over the pH range 0 to 14.

Conclusions

The following are the principal conclusions from the results of the present investigation:

(i) Using a modified cell with a 500 mesh nickel-plated gold gauze cathode the authors have extended the earlier research of Deligianni and Romankiw on surface pH measurements to nickel electrodeposition from the following electrolytes:

0.937 M, 2 M and 3 M $NiCl_2$
0.572 M $NiCl_2$ + 0.365 M $NiSO_4$
0.937 M $NiCl_2$ + 0.365 M Na_2SO_4
0.572 M $NiCl_2$ + 0.365 M $NiSO_4$–0.365 M Na_2SO_4
0.937 M $NiCl_2$ + 2 M NaCl
0.937 M $NiCl_2$ + 0.485 M H_3BO_3
0.937 M $NiCl_2$ + 1.31 M NH_4Cl

Experiments were conducted principally at 25 °C and at a bulk pH of 2.5 with the current density ranging between 60 and 760 A m^{-2}.

(ii) Adding to the limited results of previous studies, it was found that lower bulk pH, higher nickel concentration, higher temperature (up to 60 °C) and the additions of H_3BO_3 and NH_4Cl suppressed the rise of the cathode surface pH.

(iii) Evidence of the buffering action of H_3BO_3 and its enhancement of nickel deposition corroborated the results of other investigators. A buffering effect was also demonstrated by NH_4Cl.

(iv) At current densities less than 240 A m^{-2} the addition of Na_2SO_4 and NaCl also suppressed the rise of the cathode pH but to a lesser extent than in the case of H_3BO_3 and NH_4Cl.

(v) The addition of sulfate to $NiCl_2$ solutions had the effect of shifting the marked increase in the surface pH to a higher current density and reducing the current efficiency of nickel electrodeposition.

(vi) As expected the cathode surface pH was always higher than the bulk pH and at higher current densities the pH could increase to the point of $Ni(OH)_2$ precipitation.

Acknowledgements

The authors express their appreciation to Falconbridge Ltd for generous financial support of this research. Special thanks are due to Dr L.T. Romankiw at IBM's Thomas J. Watson Research Centre for providing valuable literature and information.

References

[1] E. Ovari and A. I. Rotinyan, *Sov. Electrochem.* **6** (1970) 516.
[2] A. T. Kuhn and C. Y. Chan, *J. Appl. Electrochem.* **13** (1983) 189.
[3] H. Deligianni and L. T. Romankiw, *IBM J. Res. Develop.* **37** (1993) 85.
[4] H. Deligianni and L. T. Romankiw, *in* Proceedings of the Symposium on Magnetic Materials Processes and Devices (edited by L. T. Romankiw and D. A. R. Herman, Jr.), The Electrochemical Society (1990), pp. 407–22.
[5] L. T. Romankiw, pH measurement technique on cathodes during electrolysis', Presented at SUR/FIN 1990, 9–11 July (1990).
[6] L. T. Romankiw, *in* Proceedings of the Symposium on Electrodeposition Technology, Theory and Practice

---

[‡] The pH of incipient precipitation for a 0.937 M $NiCl_2$ solution works out to be

$$K_{sp} = [Ni^{2+}][OH^-]^2 = 5.47 \times 10^{-16} \ (25\,^\circ C)$$

$$pH = \frac{1}{2} \times \log \frac{K_{sp}}{K_w^2[Ni^{2+}]} = \frac{1}{2} \times \log \frac{5.47 \times 10^{-16}}{(10^{-14})^2 \times 0.937} = 6.38$$

This pH would be reached on the cathode surface for the electrodeposition of nickel from this solution at 250 A m^{-2} and 25 °C (Fig. 6).

(edited by L. T. Romankiw and D. R. Turner), The Electrochemical Society (1987), pp. 301–25.

[7] J. Ji, Ph.D. thesis, Department of Metals and Materials Engineering, The University of British Columbia, Vancouver, BC, Canada, V6T 1Z4 (1994).

[8] R. G. Bates, 'Determination of pH, theory and practice', John Wiley & Sons, New York (1973), pp. 31 and 32.

[9] J. P. Hoare, *in* Proceedings, *op. cit*, [6], pp. 269–84.

[10] R. C. V. Piatti, A. J. Arvia and J. J. Podesta, *Electrochim. Acta* **14** (1969) 541.

[11] T. M. Florence, *Aust. J. Chem.* **19** (1966) 1343.

[12] J. P. Hoare, *J. Electrochem. Soc.* **134** (1987) 3102.

[13] J. P. Hoare, *ibid.* **133** (1986) 2491.

[14] J. Horkans, *ibid.* **126** (1979) 1861.

[15] B. V. Tilak, A. S. Gendron and M. A. Mosoiu, *J. Appl. Electrochem.* **7** (1977) 495.

[16] S. G. Mairanovskii and A. P. Churilina, *Élektrokhimiya* **12** (1970) 1857.

[17] C. F. Baes, Jr. and R. E. Mesmer, 'The Hydrolysis of cations', John Wiley & Sons, New York (1976), pp. 104–11.

[18] T. N. Ostanina, I. B. Murashova and A. V. Pomosov, *Sov. Powder Metall. Met. Ceram.* **27** (1988) 523.

[19] R. M. Khalil, *J. Appl. Electrochem.* **18** (1988) 292.

[20] K. V. Venkateswaran and K. I. Vasu, *PMAI Newsl.* **13** (1987) 12.

[21] A. Calusaru, 'Electrodeposition of metal powders', Elsevier Science, New York (1979), pp. 376–86.

[22] N. Ibl, 'Advances in electrochemistry and electrochemical engineering', vol. 2, (edited by C. W. Tobias), Interscience, New York (1962), pp. 49–143.

[23] J. Bjerrum, 'Metal ammine formation in aqueous solution', P. Haase & Son, Copenhagen, Denmark (1957), pp. 180–98.